

## Research Article

# Research on Shear Strength Parameters of the Silty Fine Sand and the Rounded Gravel Layers in Nanning City

Liming Yang,<sup>1</sup> Fan Yang ,<sup>1,2</sup> Qian Zhou,<sup>1</sup> and Guangbin Zhang<sup>3</sup>

<sup>1</sup>Guangxi Communication Design Group Co., Ltd., Nanning 530029, China

<sup>2</sup>The Key Laboratory of Road and Traffic Engineering, Ministry of Education, Tongji University, Shanghai 201804, China

<sup>3</sup>Guangxi Transportation Engineering Testing Co., Ltd., Nanning 530029, China

Correspondence should be addressed to Fan Yang; 1810506@tongji.edu.cn

Received 13 April 2023; Revised 27 October 2023; Accepted 11 November 2023; Published 30 November 2023

Academic Editor: Qian Chen

Copyright © 2023 Liming Yang et al. This is an open access article distributed under the Creative Commons Attribution License, which permits unrestricted use, distribution, and reproduction in any medium, provided the original work is properly cited.

The silty fine sand and rounded gravel layers are widely distributed in Nanning City, China. Due to the low clay content, the silty fine sand and rounded gravel layers are prone to disturbance during sampling and transportation, which affects the shear strength test results. The reasonable determination of their shear strength is significant and imperative to the project. The rail transit project in Nanning is under large-scale construction. This work obtained the shear strength of the silty fine sand and the rounded gravel layers by conducting laboratory tests on undisturbed samples from deep foundation pits, combined with large-scale direct shear in situ tests. In addition, geotechnical investigation reports for typical projects in Nanning City were compiled, and the test data for the silty fine sand and the rounded gravel layers were comparatively analyzed using the empirical value. The results show that the shear strength test values of the fine sand layer are consistent with the current standard empirical values, and empirical values can be used for reference. The shear strength test value of the rounded gravel layer has significantly improved compared to the current standard empirical value, with a cohesion ( $c$ ) value of 0–6.8 kPa and an increase in internal friction angle ( $\varphi$ ) of 0%–12.5%. It is recommended to determine the shear strength of the rounded gravel layer based on the actual situation.

## 1. Introduction

For a long time, the determination of the physical and mechanical parameters of rock and soil layers has been a technical difficulty in the field of geotechnical engineering. Using different instruments, different test methods, and statistical analysis, some scholars conducted numerous studies on the accurate value of the physical and mechanical parameters of rock and soil layers [1–10]. The determination of the shear strengths of the silty fine sand and the rounded gravel layers is very important to geotechnical investigations and design. The value used in the actual project is generally obtained from laboratory tests and through engineering experience, and thus the value used contains a significant amount of uncertainty [11].

A large number of studies have been conducted on the silty fine sand and the rounded gravel layers. Hu et al. [12] conducted a series of true triaxial tests on the Shanghai silty fine sand for different coefficients of intermediate principal stress using a flexible true triaxial apparatus. Based on these

tests, the shape function of the Mohr–Coulomb strength criterion was improved, and the improved function was validated by the tests. The results demonstrated that the strength criterion under triaxial conditions reflects the true stress state of silty fine sand better. Hassan et al. [13, 14] studied the mechanical properties of different soils through multiple triaxial compression tests and interface direct shear tests and found that the performance of geosynthetic reinforcement in lower plastic soil is better than that in higher plastic soil. Nawaz et al. [15] established an unconfined compressive strength (UCS) prediction model with a common influence on soil properties using gene expression programming and found that liquid limit and fine particle content are the most sensitive parameters affecting UCS, while sand content is the least critical parameter. Cabalar et al. [16] and Cabalar and Hasan [17] studied 10–19 mm angular and circular aggregates. The California bearing ratio (CBR) and UCS ratio tests were carried out on the mixture of clay and two aggregates with different contents. It was found that the maximum dry

density, UCS, and CBR value of the mixture containing rounded gravel were higher than those of the mixture containing angular gravel, and the optimal water content was lower. Thevanayagam et al. [18] analyzed the large strain undrained shear strength of silty fine sand under triaxial compression and proposed the standard of undrained shear strength behavior of silty fine sand according to the relative compaction percentage applied in the field. Ecemis and Karaman [19] and Monkul and Ozden [20] studied the effect of fine particle content on the mechanical properties of clayey sand and found that fine particle content has a significant impact on its compression performance and liquefaction resistance. Kong et al. [21] conducted in-depth research on the shear strength of conglomerate soil under different water contents. A large-scale direct shear test was conducted on circular gravel soil in the plateau alluvial-lacustrine deposit, and the shear strength curves and water content curves of the circular gravel soil under natural and saturated conditions were obtained, providing a certain reference for optimizing engineering design parameters. Chang and Phantachang [22] studied the effect of gravel content on the shear properties of gravelly soils and found that the shear strength of gravelly soils depends on the stacking conditions of the main particles, while the drainage shear strength of loose gravel sand is mainly affected by the properties of the sand matrix. Tang et al. [23] conducted a large-scale triaxial test to determine the mechanical parameters of two kinds of rounded gravel soil with different degrees of compactness from Nanning City. In the laboratory test, only the disturbed samples of rounded gravel could be measured. After the undisturbed samples were screened, grains from other sub-way stations were used to make the test samples. Because of this, there were some differences between the test results and the real results. Zhang [24] studied the strata formation combination model and the division along Nanning Rail Transit Line 1, but only the heavy dynamic penetration test was conducted on the rounded gravel layer, while the strength of the rounded gravel layer was not studied. Previous literature has researched the shear strength of the silty fine sand and rounded gravel layers. However, the shear strengths of the silty fine sand and the rounded gravel layers are obtained through traditional laboratory testing using a silty fine sand core sample extracted by drilling. However, due to the low clay content of the silty fine sand and the rounded gravel, it is extremely easy to cause disturbance during core sample extraction and transportation. Therefore, the samples for laboratory tests are generally disturbance samples rather than undisturbed samples, resulting in errors between the test results and the actual values.

The excavation of a large number of deep foundation pits in the construction of rail transit in Nanning City has extensively exposed the silty fine sand and the rounded gravel layers. This work adopted the in situ testing method, which directly conducts large-scale shear tests on the undisturbed samples on site to obtain the shear strength of the silty fine sand and the rounded gravel layers. The shear strength laws of the silty fine sand and the rounded gravel layers were summarized. A method for determining shear strength was

proposed based on a comparative analysis of laboratory test results, large triaxial test data, statistical analysis of investigation data, and recommended values in standard specifications. Up to now, the research results of this paper have been successfully applied to the design and construction of the main body and auxiliary structures of stations in 43 silty sand layers and rounded gravel layers of Nanning Metro Lines 1–5 and have been included in the local standard of Guangxi Engineering Construction (DBJ/T45-065-2018) [25].

## 2. Geological Background Analysis

Nanning City is located in the Nanning Basin, which increases in elevation from the northeast to the southwest and is surrounded by hills. The urban area is located on the relatively flat Yongjiang River terrace and on the peneplain accumulated along the rivers. The terrain is relatively open and flat, as shown in Figure 1. According to Pan [26], there are five Yongjiang River terraces in Nanning City, which have a well-preserved binary structure and cover a large area. The stratigraphy and lithology of the urban area are complex and contain widely distributed Quaternary alluvium, which is composed of mud, mucky soil, clay, silty clay, silt, silty fine sand, fine sand, medium sand, coarse sand, gravel sand, rounded gravel, and pebbles; Quaternary eluvial clay and silty clay; Neocene mudstone, siltstone, and coal seams; and Paleogene sandstone, argillaceous siltstone, and mudstone. The neotectonic movement in Nanning City is characterized by the slow uplift of the crust and the incision of the river valley, which is mainly manifested in the following aspects: the faults along the margin and in the interior of the Paleogene syncline basin cut the Paleogene strata, slight bending of Quaternary sediments and faults, and terraces I–IV on both sides of the Yongjiang River were created by the uplift of the crust and the incision of the river valley since the Quaternary [27]. According to the Zoning Map of China's Seismic Peak Acceleration (1 : 4 million), the seismic peak acceleration in the study area is 0.05 g, which is equivalent to a basic seismic intensity of VI. The groundwater in the Nanning Basin is generally divided into four categories: pore water in loose rocks, pore fissure water in clastic rocks, bedrock fissure water in carbonate rocks, and fissure cave water in carbonate rocks.

## 3. Test Methods

**3.1. On-Site Direct Shear Test.** According to the GB 50307-2012 standard [28], an on-site direct shear test (in situ test) was conducted on the silty fine sand and rounded gravel layers. The specific steps are as follows: (1) in the excavation test pit, samples were prepared according to the size of the shear box (70.7 cm × 70.7 cm × 35 cm), and the size of the shear surface opening was determined by the minimum particle size of the soil layer measured on site, which is one-fourth to one-third of the minimum particle size. (2) Pressurization, reaction devices, and sensors were installed. To ensure the water saturation of the sample, a certain amount of water was poured into the test pit so that the water surface in the

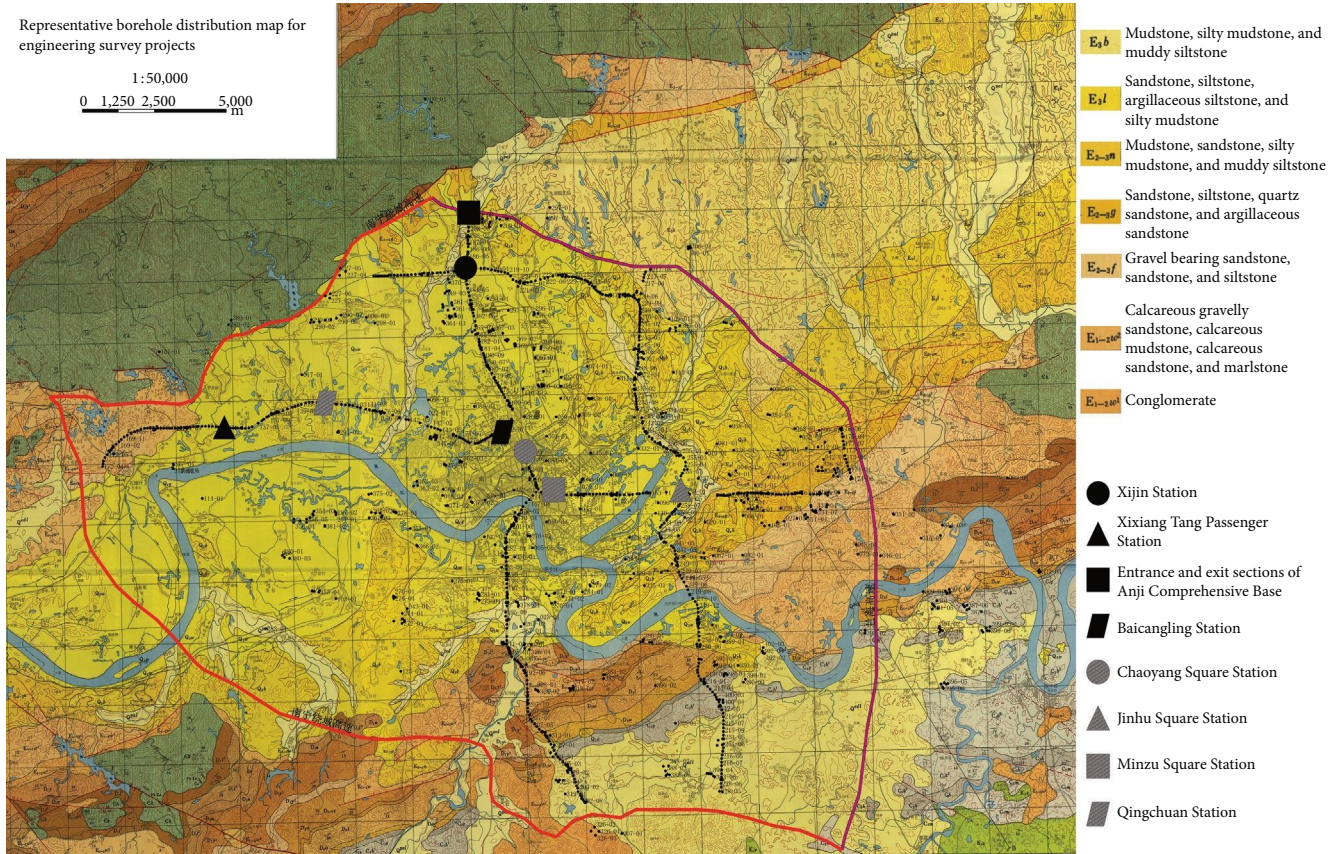


FIGURE 1: Geological background map of Nanning City and sampling sites location.

test pit was above the shear plane. (3) The maximum normal load was 300 kN, applied in four to five levels to the maximum normal load, i.e., each load level was 60–75 kN. Record the dial indicator reading every 5 min. The next level could be applied when the change within 5 min was less than 0.05 mm. (4) After the maximum normal load stabilizes, the shear load was applied in stages with a maximum shear load of 200 kN. The shear load at each level was approximately 8%–10% of the estimated maximum shear load, which was 16–20 kN. Apply a load level every 30 s, and when the shear deformation increases sharply or reaches 1/10 of the specimen size (i.e., 7.07 cm), terminate the test and record the maximum shear load. Each group of experiments consists of three specimens.

**3.2. Fast Shear Test.** According to the GB/T 50123-2019 specification [29], a fast shear test (laboratory test) was carried out on the silty fine sand and rounded gravel layers. The steps are as follows: (1) pour 1,200 g of representative air-dried sand sample screened through a 2 mm sieve into the shear box as required. (2) Turn the hand wheel to make the steel ball at the front end of the shear box contact the load sensor or force meter, and adjust the load sensor or force meter reading to zero. (3) Conduct shear tests under four different vertical pressures (100, 200, 300, and 400 kPa), each of which can be lightly applied once. (4) After applying vertical pressure, immediately remove the fixing pin. Shear the sample at a rate of 0.8–1.2 mm/min, resulting in shear loss

within 3–5 min. When the reading of shear stress was stable or had a significant retreat, it indicates that the sample has been sheared, and it was advisable to shear until the shear deformation reached 4 mm. When the reading of shear stress continues to increase, the shear deformation shall reach 6 mm, and the reading of the load sensor or force meter shall be measured until the shear is damaged. Each group of experiments consists of four specimens.

The shear stress of the sample is calculated as follows:

$$\tau = \frac{CR}{A_0} \times 10, \quad (1)$$

where  $\tau$  is the shear stress (kPa),  $C$  is the calibration coefficient of the force meter (N/0.01 mm),  $R$  is the reading of the force meter (0.01 mm), and  $A_0$  is the initial area (cm<sup>2</sup>).

## 4. Results and Discussion

**4.1. Mechanical Properties of the Silty Fine Sand Layer.** The shear strength of the silty fine sand layer was analyzed by fast shear test and in situ direct shear test. Based on the statistical analysis of 71 engineering survey data of Nanning Rail Transit Lines 1 and 2, various test results and specification values were compared, and the method for determining the shear strength of silty fine sand layer was proposed.

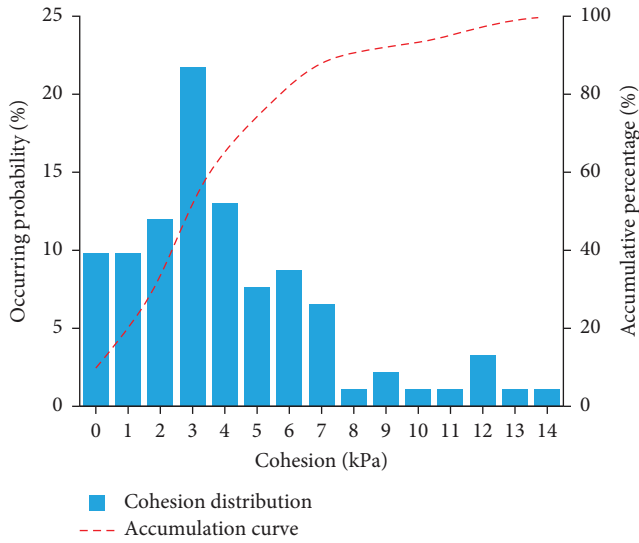


FIGURE 2: Histogram of the cohesion distribution of the silty fine sand.

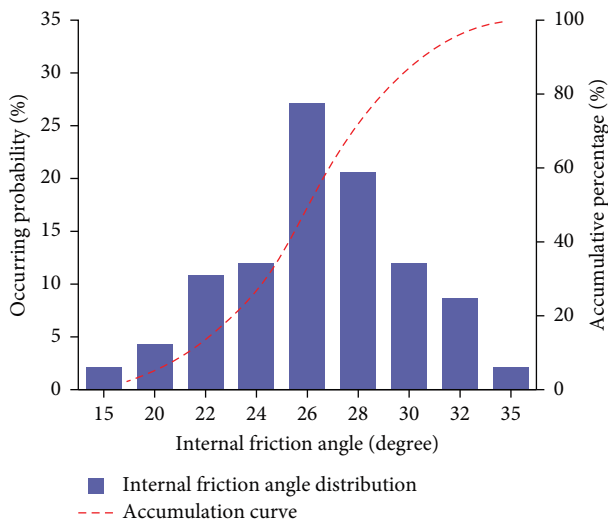


FIGURE 3: Histogram of the internal friction angle distribution of the silty fine sand layer.

**4.1.1. Laboratory Test.** Ninety-two groups of undisturbed samples were collected from 11 Nanning rail transit stations for the laboratory test. Fast shear tests were carried out to obtain the shear strength index of the silty fine sand. Figures 2 and 3 show the distribution histograms of the cohesion ( $c$ ) and the internal friction angle ( $\varphi$ ) of the shear strength of the silty fine sand, respectively. Table 1 presents the statistics of the shear strength indices of the silty fine sand.

As can be seen in Table 1, the maximum cohesion of the silty fine sand in Nanning is 14.2 kPa, the minimum cohesion is 0 kPa, and the mean cohesion is 4.5 kPa. The cohesion of 89% silty fine sand shall not exceed 7 kPa. This result is consistent with Cabalar et al.'s [16] and Cabalar and Hasan's [17] researches. The reason is that there is little or no clay in the silty fine sand from Nanning City, and the interaction

between sand particles is small, which shows that the cohesion is generally small in the macroview. In addition, the maximum internal friction angle of silty fine sand is  $33.4^\circ$ , the minimum value is  $12.1^\circ$ , and the average value is  $25.3^\circ$ . The probability distribution of the internal friction angle meets the trend of normal distribution, and the proportion of  $22^\circ$ – $30^\circ$  exceeds 82%. The physical properties of the silty fine sand mainly determine this.

**4.1.2. In Situ Test.** During the excavation of the deep foundation pits for the Nanning rail transit stations, a large area of the silty fine sand layer was exposed, which is conducive to in situ testing of the silty fine sand layer. Three rail transit stations, i.e., the Xijin Station, the Xixiang Tang Passenger Station, and the Anji Comprehensive Base, which have a thick silty fine sand layer, were selected for on-site direct shear testing. The on-site situation is shown in Figure 4.

In order to obtain a more accurate shear strength index and to reduce the discreteness of the test data, a shear box with an area of  $0.5 \text{ m}^2$  (side length of about 70.7 cm and height of 35 cm) was used in the test. The reaction system relied on the deep foundation pits to support the continuous walls and jacks to support the heaped load or ground anchor. When the test location was far away from the continuous wall, the heaped load method was used to provide horizontal and vertical reactions (Figure 5). When the testing was conducted near the continuous wall, the horizontal reaction was provided by the continuous wall, and the vertical reaction was provided by the ground anchor (Figure 6). According to the size of the in situ test area and the distribution of the silty fine sand, two groups, two groups, and five groups of in situ shear tests were carried out in the entrance and exit sections of Xijin Station, Xixiang Tang Passenger Station, and Anji Comprehensive Base, respectively. The results are reported in Table 2.

The mean cohesion of the silty fine sand layer is 2.05 kPa, and the mean internal friction angle is  $27.3^\circ$ . From the regional point of view, the cohesion at the entrance and exit sections of Xijin Station is 0.07–0.58 kPa, and the internal friction angle is  $21.3^\circ$ – $23.2^\circ$ ; the cohesion at Xixiang Tang Passenger Station is 0 kPa, and the internal friction angle is  $22.2^\circ$ – $23.9^\circ$ ; the cohesion at Anji Comprehensive Base is 0.97–7.07 kPa, and the internal friction angle is  $23.3^\circ$ – $26.1^\circ$ . The silty fine sand at the entrance and exit sections of Anji Comprehensive Base is relatively dense and contains many cohesive particles. The internal friction angle decreases first and then increases with the increase of fine particle content. When the content of fine particles is low, coarse particles hinder the mutual sliding between soil particles during shearing, improving the strength of the soil sample, and the internal friction angle is relatively large. Once the content of fine particles increases, the gaps between the coarse particles are filled with fine particles, and the coarse particles are evenly distributed around the fine particles. Shear also mainly moves around the fine particles, weakening the role played by the coarse particles. Therefore, the internal friction angle decreases with the increase of fine particle content, which is consistent with Cabalar et al.'s [16]

TABLE 1: Laboratory test results of the shear strength of the silty fine sand.

Results	Maximum	Minimum	Mean	Total sample size	Statistical number	Standard deviation	Coefficient of variation
$c$ (kPa)	14.2	0	4.5	92	87	3.22	0.71
$\varphi$ ( $^{\circ}$ )	33.4	12.1	25.3	92	87	3.74	0.15

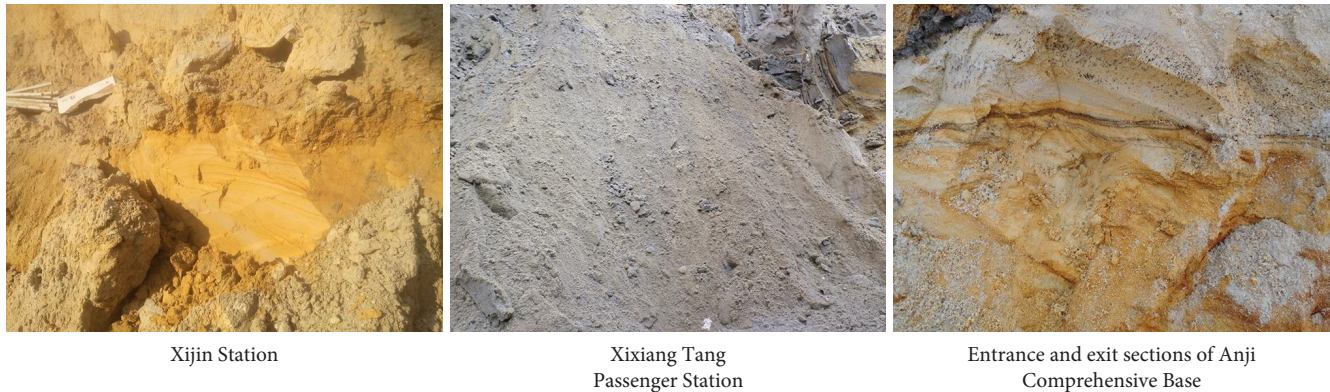


FIGURE 4: Three testing points on-site situation.



FIGURE 5: Reaction provided by the heaped load.



FIGURE 6: Reaction provided by the ground anchor.

and Cabalar and Hasan's [17] researches and previous survey data. When the content of fine particles increases to a certain critical value, many fine particles have viscosity, which, to some extent, hinders the shear process.

The compactness of sand has an essential impact on its engineering properties. When the sand is dense, the structure

is relatively stable, with less compressibility and greater strength, making it a good building foundation. When in a loose state (especially for fine sand), it has poor stability, high compressibility, and low strength, belonging to weak soil. Under certain confining pressure, the stress-strain relationship of loose sand exhibits a strain-hardening type, and its volume gradually decreases, exhibiting a certain degree of shear shrinkage. The shear stress increases with the increase of shear strain and finally tends to a constant strength called residual strength. The stress-strain relationship of dense sand exhibits a strain softening type, with its volume initially decreasing slightly and then increasing beyond its initial volume, exhibiting a certain degree of shear dilation. As the confining pressure increases, the shear behavior of sand will exhibit shear shrinkage. The shear stress gradually increases to its peak at the beginning and then gradually decreases until it reaches residual strength. The internal mechanism of the above phenomenon is that when loose sand is subjected to shear, particles roll down to new equilibrium positions in the pores, resulting in a more compact arrangement of particle structures and a reduction in volume, thus exhibiting shear shrinkage. On the contrary, for dense sand, under shear force, particles will rotate around adjacent particles and climb upwards, leading to volume expansion and exhibiting shear dilation. As the confining pressure increases, particles will roll back into new pores, the volume of sand will decrease, and it will also exhibit shear shrinkage.

**4.1.3. Statistical Analysis.** The empirical values of the physical and mechanical parameters of the rock and soil mass are obtained by the engineering construction personnel using laboratory tests, in situ tests, and engineering analogy. Therefore, it is representative. For example, Hassan et al. [30, 31] evaluated the subsoil data in 210 geotechnical investigation reports based on soil type, standard penetration

TABLE 2: Results of the direct shear test on the silty sand layer.

Results	Test site number	Moisture content (%)	Natural density ( $\text{g}\cdot\text{cm}^{-3}$ )	Void ratio	$c$ (kPa)	$\varphi$ ( $^\circ$ )	Compactness
Xijin Station	1	13.9	1.69	0.6	0.07	21.3	Loose
	2	10.9	1.83	0.79	0.58	23.2	Slightly dense
Xixiang Tang Passenger Station	1	8.7	1.52	0.924	0	22.2	Loose
	2	28.7	1.68	0.848	0	23.9	Slightly dense
Entrance and exit sections of Anji Comprehensive Base	1	20.5	1.94	0.634	7.07	24.5	Slightly dense
	2	22.7	1.93	0.685	1.62	25.8	Moderately dense
	3	20.3	2.00	0.564	0.97	23.3	Moderately dense
	4	21.2	1.89	0.680	1.56	23.3	Moderately dense
	5	12.7	1.74	0.710	6.57	26.1	Slightly dense

TABLE 3: Empirical values of the mechanical parameters of the silty fine sand in Nanning.

Results	Direct fast shear		Consolidated fast shear	
	$c$ (kPa)	$\varphi$ ( $^\circ$ )	$c$ (kPa)	$\varphi$ ( $^\circ$ )
Maximum	0	30	0	30
Minimum	0	16	0	29
Mean	0	24.4	0	29.5
Total sample size	71		71	
Statistical number	56		13	
Standard deviation	0	3.7	0	0.52
Coefficient of variation	0	0.15	0	0.008

(SPT-N value), undrained shear strength, and consolidation parameters and used spatial interpolation method to create soil zonation maps. The correlation coefficient of the predicted SPT-N value is about 85%, while that of soil type is 94%. It has an excellent guiding role in quickly evaluating the stiffness and strength of the subsoil during the preliminary planning and feasibility study process of construction projects. As the research object of this work is only shear strength, the statistical analysis of parameters mainly revolves around relevant parameters such as cohesion and internal friction angle.

More than 70 copies of the engineering investigation data for Nanning Rail Transit Lines #1 and #2 were collected. According to the analysis and selection of the geotechnical parameters regulated by the code for investigation of geotechnical engineering (GB 50021-2001) [32], the mean, standard deviation, coefficient of variation, range of the data distribution, and the quantity of data of the geotechnical parameters are provided in the geotechnical engineering investigation reports, and the statistical analysis was conducted on each geotechnical parameter of the rock and soil masses in the foundation pits of the rail transit. The statistical results are reported in Table 3.

According to Table 3, the number of samples used in the statistical analysis of the direct fast shear test reached 56, and the cohesion values of the samples are all 0 kPa. The internal friction angles are  $16^\circ$ – $30^\circ$ , with a mean of  $24.4^\circ$ . The number of samples used in the statistical analysis of the

consolidated fast shear is 13, and the cohesion values of the samples are all 0 kPa. The internal friction angles are  $29^\circ$ – $30^\circ$ , with a mean of  $29.5^\circ$ . Due to the dissipation of the pore water pressure and the increase in the effective stress during consolidation, the internal friction angle obtained from the consolidated fast shear test is slightly larger than that obtained from the direct fast shear test.

*4.1.4. Comparison of the Shear Strengths.* The local standards and the geological engineering manual for Guangdong Province and Hubei Province near Guangxi were compared. Table 4 shows the compiled relevant indexes.

In Table 4, the strength parameters of the silty fine sand from the different areas are quite different. As stated in the code for foundation pit support in Hubei Province, the strength index of the silty fine sand is closely related to the standard penetration test blow count, and its internal friction angle is slightly larger than that of the Nanning in situ test. As stated in the “Code for Foundation Pit Support in Guangdong Province,” the internal friction angle of the fine sand is  $25^\circ$ – $32^\circ$ , which is larger than that of the Nanning in situ test. The silty fine sand is subdivided into fine sand, silty sand, and ultrafine sand for use in geotechnical engineering. The internal friction angle is  $26^\circ$ – $36^\circ$ , which is larger than that of the in situ test. Based on the standard penetration test blow count and porosity, the “Geological Manual for Water Conservancy and Hydropower Engineering” reports the empirical values of the internal friction angle of fine sand and ultrafine sand, which are basically consistent with those of the in situ test on silty fine sand carried out in Nanning.

As seen in Tables 1–4, the statistical results of the laboratory test are close to those of the empirical values presented in the rail transit investigation report. The mean internal friction angle ( $\varphi$ ) of the laboratory test is  $0.9^\circ$ , which differs from the mean empirical value presented in the investigation report. The cohesion of the silty fine sand in the laboratory test exhibits a certain dispersion, and the coefficient of variation reaches 0.71. The analysis shows that the main cause of the large dispersion of the results is the large difference in the silt content. The cohesion and internal friction angle of the silty fine sand layer obtained in the in situ test are smaller than those obtained from the laboratory test, those in the investigation report data, and the relevant local standards.

TABLE 4: Strength parameters of the silty fine sand reported in the current regulations.

Source	Soil type	Relevant indexes	Shear stress index $c$ (kPa)	$\varphi$ ( $^{\circ}$ )
Code for foundation pit support in Hubei Province	Silty and fine sand	Standard penetration test blow count	10	27
			14	30
			21	33
			30	35
		40	36	
Code for foundation pit support in Guangdong Province	Fine sand	Compactness	Loose	25–28.5
			Slightly dense	29–32
Rock and soil engineering	Fine sand	Compactness	Loose	28
			Slightly dense	30
			Moderately dense	34
			Dense	36
	Silty sand	Compactness	Loose	26
			Slightly dense	28
			Moderately dense	32
	Ultrafine sandy soil	Compactness	Dense	34
			Moderately dense	28–32
			Dense	30–34
Geological manual for water conservancy and hydropower engineering	Fine sand, ultrafine sand	Standard penetration test blow count	4	20
			5	22
			6	24
			7	26
	Fine sand, ultrafine sand	Void ratio	8	28
			0.8	26
			0.7	28
			0.6	32
		0.5	34	

TABLE 5: Results of the direct shear test on the rounded gravel layer.

Test site	Test site number	Moisture content (%)	Natural density ( $\text{g}\cdot\text{cm}^{-3}$ )	Permeability coefficient (m/d)	$c$ (kPa)	$\varphi$ ( $^{\circ}$ )	Compactness
Baicangling Station	1	47.3	2.01	90	6.7	31.0	Moderately dense
Chaoyang Square Station	1	51.8	2.05	85	2.0	31.0	Moderately dense
	2	49.7	2.14	87	6.8	34.2	Dense
	3	50.3	2.16	81	4.5	33.0	Dense
Jinhu Square Station	1	50.2	1.91	71	0.2	28.7	Slightly dense
	2	48.9	2.04	74	0.0	30.0	Moderately dense
Minzu Square Station	1	49.1	2.08	54	0.0	27.0	Moderately dense
	2	51.4	2.15	61	0.0	29.5	Dense
Qingchuan Station	1	51.7	2.13	80	0.0	36.9	Dense

**4.2. Mechanical Properties of Rounded Gravel Layer.** The shear strength of the rounded gravel layer was analyzed by in situ direct shear test. One hundred fourteen engineering investigation data of Nanning Rail Transit Lines 1–3 were statistically analyzed, and the in situ test results were compared with the literature data. Finally, a method for determining the shear strength of the rounded gravel layer was proposed.

**4.2.1. In Situ Test.** The large-scale direct shear test method described in Section 3.1 was used for the in situ field shear tests at the Baicangling, Chaoyang Square, Jinhu Square, Minzu Square, and Qingchuan stations of the Nanning rail transit system, and the direct shear test results of the rounded gravel layer were obtained (Table 5).

As can be seen from Table 5, the mean cohesion of the rounded gravel layer is 2.2 kPa, and the mean internal friction angle is  $31.3^{\circ}$ . Divided by station, the cohesion of Chaoyang Square Station is 2.0–6.8 kPa, and the internal friction angle is  $31.0^{\circ}$ – $34.2^{\circ}$ ; the cohesion of Jinhu Square Station is 0–0.2 kPa, and the internal friction angle is  $28.7^{\circ}$ – $30.0^{\circ}$ ; the cohesion of Minzu Square Station is 0 kPa, and the internal friction angle is  $27^{\circ}$ – $29.5^{\circ}$ ; the cohesion of Baicangling Station is 6.7 kPa, and the internal friction angle is  $31.0^{\circ}$ ; and the cohesion of Qingchuan Station is 0 kPa, and the internal friction angle is  $36.9^{\circ}$ . From the above data, it can be seen that there are certain differences in the cohesion of the rounded gravel layer in different regions. The reason is that different rounded gravel layers contain different clay content, such as the higher clay content at Baicangling Station and Chaoyang Square Station, which makes their cohesion greater than in other areas. The internal friction angle data show that the internal friction angle of the rounded gravel layer in these five regions ranges from  $27^{\circ}$  to  $37^{\circ}$ , and the difference is small, indicating that the properties of the rounded gravel layer in these regions are relatively uniform.

**4.2.2. Statistical Analysis of the Recommended Values of the Mechanical Parameters.** The recommended values of the physical and mechanical parameters of the rock and soil mass were obtained by engineering construction personnel using laboratory tests, in situ field tests, and engineering

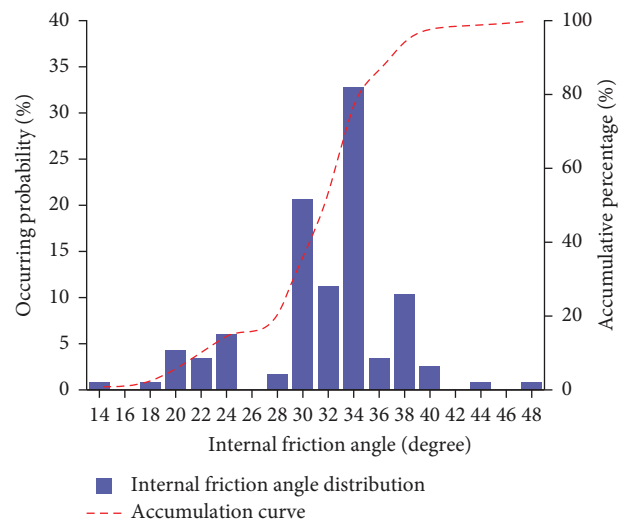


FIGURE 7: Histogram of the frequency distribution of the internal friction angle ( $\varphi$ ) of the rounded gravel layer.

analogy. Therefore, they are representative. Statistical analysis was conducted on the strength parameters of 114 collected items to assess the physical and mechanical recommended values of the rock and soil mass in the investigation reports of rail transit lines #1, #2, and #3, which can reflect the strength of the rounded gravel layer better. Figure 7 shows the histogram of the internal friction angle frequency distribution of the rounded gravel layer. Table 6 shows the statistical results of the recommended values of the mechanical parameters.

As shown in Table 6, the recommended cohesion value of the rounded gravel layer is 0 kPa, except for some nonzero values, indicating that the rounded gravel layer contains no clay or only a very small amount of clay. Based on the statistical analysis of the internal friction angle, the distribution of the internal friction angle is relatively concentrated. Most of the angles fall within the range of  $30^{\circ}$ – $36^{\circ}$ , and they are mostly concentrated within the range of  $34^{\circ}$ – $36^{\circ}$ . The internal friction angles of the rounded gravel layer for 40 construction projects fall within the range of  $34^{\circ}$ – $36^{\circ}$ .



TABLE 6: Recommended values of the mechanical parameters of the rounded gravel.

Results	Maximum	Minimum	Mean	Total sample size	Statistical number	Standard deviation	Coefficient of variation
$c$ (kPa)	10	0	0.3	114	114	1.48	4.93
$\varphi$ (°)	48	15	32.5			5.34	4.93

TABLE 7: Comparison of the strength parameters of the rounded gravel.

Methods	Compactness	Test site	$c$ (kPa)	$\varphi$ (°)
In situ test	Moderately dense	Baicangling Station	6.7	31.0
	Moderately dense	Chaoyang Square Station	2.0	31.0
	Moderately dense	Jinhu Square Station	0.2	30.0
	Moderately dense	Minzu Square Station	0.0	27.0
Large-scale triaxial test	Moderately dense	North bank of Baisha Bridge	0.0	41.0
In situ test	Dense	Chaoyang Square Station	6.8	34.2
	Dense		4.5	33.0
	Dense	Minzu Square Station	0.0	29.5
	Dense	Qingchuan Station	0.0	36.9
Large-scale triaxial test	Dense	North bank of Baisha Bridge	0.0	45.0
Mean	–	–	0.3	32.5

TABLE 8: Empirical values of the strength indices of the rounded gravel layer in Nanning.

$c$ (kPa)	$\varphi$ (°)	Project	Data source
0	30	Science and technology business building of Guangxi Bureau of geology and mineral prospecting and exploitation	Wei et al. [33]
–	48	A high-rise building in Nanning	Wu [34]
–	30	95,072 army staff residence	Wu [34]
5	28	Nanning Xiguan square project	Mai [35]
0	30	Nanning rail transit project	Huang and Yang [36]
–	33	A high-rise building in Nanning	Zhou [37]

4.2.3. *Comparison of the Shear Strengths.* Tang et al. [23] used the TAJ-2000 large-scale dynamic and static triaxial apparatus at the Dynamic and Static Triaxial Laboratory of Wuhan Institute of Geotechnical Mechanics, Chinese Academy of Sciences, to test a rounded gravel soil sample from the node traffic control project on the north bank of Baisha Bridge, Nanning City. The results were compared with the results of the in situ shear test and the statistical analysis results of the recommended values presented in the rail transit investigation report, which provided us with a more rational understanding of the strength parameters of the rounded gravel layer.

The large-scale triaxial test is an indoor simulation test, and the on-site direct shear test is an in situ test. The test principles and steps are similar, and the test results and analysis methods are consistent. This work compared the shear parameters obtained by two methods. Table 7 shows the comparative analysis of the strength parameters of the rounded gravel layer. The cohesion of the moderately dense rounded gravel layer obtained from the in situ test is 0–6.7 kPa, and the internal friction angle is 27°–31.0°. The cohesion of the rounded gravel layer obtained from the large-

scale triaxial test is 0 kPa, and the internal friction angle is 41.0°. Therefore, the internal friction angle of the rounded gravel layer obtained from the large-scale triaxial test is larger. The cohesion of the dense rounded gravel layer obtained from the in situ test is 0–6.8 kPa, and the internal friction angle is 29.5°–36.9°. The cohesion of the rounded gravel layer obtained from the large-scale triaxial test is 0 kPa, and the internal friction angle is 45.0°. Therefore, the internal friction angle of the rounded gravel layer obtained from the large-scale triaxial test is larger. According to the statistical value of the recommended value presented in the investigation report, the mean cohesion  $c$  is 0.3 kPa, and the internal friction angle is 32.5°.

As the compactness of the rounded gravel layer increases, the internal friction angle increases. The main reason for this is that as the density of the rounded gravel layer increases, the number of contact points in the soil increases. In addition, the connection between the soil masses becomes tighter, and the internal friction angle of the soil becomes larger. Similarly, when using the large-scale triaxial test equipment, due to the existence of the circumferential surrounding rocks, the soil was compacted, so the void ratio was reduced,

and the internal friction angle was increased, which resulted in the internal friction angle obtained from the large-scale indoor triaxial apparatus being larger than that obtained from the in situ test.

The empirical values of the strength index of the rounded gravel layer in Nanning City have been reported in previous studies (Table 4). The strength index of the rounded gravel layer in Nanning City is smaller than that obtained from the in situ field test. The rounded gravel layer was not disturbed in the in situ test, while the values in Table 8 exhibit various degrees of disturbance, so the strength is reduced to a certain extent.

## 5. Conclusions

This work tested the shear strength parameters of the silty fine sand and the rounded gravel layer through laboratory, in situ, and large-scale triaxial tests and compared them with the empirical and recommended values of standard specifications. This paper provides a reference for the values of shear strength parameters of the silty fine sand and the rounded gravel layers in Nanning City, and the results have been applied to actual subway projects. The following conclusions were drawn:

- (1) The content of clay particles in the silty fine sand layer is generally low, and the cohesion is minor or even 0. The cohesion can be taken as 0–7.07 kPa. The internal friction angle increases with the increase of compactness and can be taken as 21.3°–26.1°. The in situ test results are consistent with the recommended values in the standard specifications. The shear strength index can refer to the current effective standard specifications.
- (2) The shear strength index test values of the rounded gravel layer obtained through the in situ test have significantly improved compared to the current effective standard empirical values. The cohesion can be taken as 0–6.8 kPa, and the internal friction angle can increase by 0%–12.5% (taking 27.0°–36.9°). Therefore, it is recommended to refer to empirical values for values based on actual situations, such as the size of confining pressure, support structure form, and compactness.
- (3) The shear strength index obtained by conducting large-scale direct shear tests on the undisturbed samples on site is closest to the actual situation of the soil layer. If conditions permit, especially the shear strength index of the rounded gravel layer should be obtained through in situ testing. If conditions do not allow, priority should be given to using large-scale triaxial tests or ordinary triaxial tests to obtain shear strength parameters.

## Data Availability

The data used to support the findings of this study are available from the corresponding author upon request.

## Conflicts of Interest

The authors declare that there are no conflicts of interest regarding the publication of this paper.

## Acknowledgments

This study was sponsored by the Guangxi Science and Technology Research Program (Gui Ke Gong 14124004-4-13) and the Key R&D Program of Guangxi (GUI KE AB20159036).

## References

- [1] K. Tian, H. Zhang, and B. Luo, "Development of a new-type apparatus for measuring seepage deformation," *Chinese Journal of Rock Mechanics and Engineering*, vol. 27, no. S2, pp. 3441–3444, 2008.
- [2] Y. F. Chen, Z. Y. Ai, Z. G. Ma, and Z. K. Ye, "Vertical performance of rock-socketed pile group in layered saturated rock-soil mass," *Computers and Geotechnics*, vol. 157, Article ID 105322, 2023.
- [3] E. Kanari, P. Barré, F. Baudin et al., "Predicting Rock-Eval<sup>®</sup> thermal analysis parameters of a soil layer based on samples from its sublayers; an experimental study on forest soils," *Organic Geochemistry*, vol. 160, Article ID 104289, 2021.
- [4] C. Su, P. Wang, M. Zhao, G. Zhang, and X. Bao, "Dynamic interaction analysis of structure–water–soil–rock systems under obliquely incident seismic waves for layered soils," *Ocean Engineering*, vol. 244, Article ID 110256, 2022.
- [5] Y. Yang, G. Sun, H. Zheng, and C. Yan, "An improved numerical manifold method with multiple layers of mathematical cover systems for the stability analysis of soil–rock-mixture slopes," *Engineering Geology*, vol. 264, Article ID 105373, 2020.
- [6] W. Shen, T. Zhao, F. Dai, M. Jiang, and G. G. D. Zhou, "DEM analyses of rock block shape effect on the response of rockfall impact against a soil buffering layer," *Engineering Geology*, vol. 249, pp. 60–70, 2019.
- [7] Y. Zhao and Z. Liu, "Study of material composition effects on the mechanical properties of soil–rock mixtures," *Advances in Civil Engineering*, vol. 2018, Article ID 3854727, 10 pages, 2018.
- [8] M. Paliwal, H. Goswami, A. Ray, A. K. Bharati, R. Rai, and M. Khandelwal, "Stability prediction of residual soil and rock slope using artificial neural network," *Advances in Civil Engineering*, vol. 2022, Article ID 4121193, 14 pages, 2022.
- [9] Y. Zhao and Z. Liu, "Numerical experiments on triaxial compression strength of soil–rock mixture," *Advances in Civil Engineering*, vol. 2019, Article ID 8763569, 15 pages, 2019.
- [10] W. Wu, Y. Yang, H. Zheng, S. Wang, N. Zhang, and Y. Wang, "Investigation of the effective hydro-mechanical properties of soil–rock mixtures using the multiscale numerical manifold model," *Computers and Geotechnics*, vol. 155, Article ID 105191, 2023.
- [11] X. Li, Q. Liao, J. He, and J. Chen, "Study on in-situ tests of mechanical characteristics on soil–rock aggregate," *Chinese Journal of Rock Mechanics and Engineering*, vol. 26, no. 12, pp. 2377–2384, 2007.
- [12] P. Hu, M. Huang, S. Ma, and X. Lü, "True triaxial tests and strength characteristics of silty sand," *Rock and Soil Mechanics*, vol. 32, no. 2, pp. 465–470, 2011.
- [13] W. Hassan, K. Farooq, H. Mujtaba et al., "Experimental investigation of mechanical behavior of geosynthetics in

- different soil plasticity indexes,” *Transportation Geotechnics*, vol. 39, Article ID 100935, 2023.
- [14] W. Hassan, B. Alshameri, M. N. Nawaz, and S. U. Qamar, “Experimental study on shear strength behavior and numerical study on geosynthetic-reinforced cohesive soil slope,” *Innovative Infrastructure Solutions*, vol. 7, Article ID 349, 2022.
- [15] M. N. Nawaz, S.-H. Chong, M. M. Nawaz, S. Haider, W. Hassan, and J.-S. Kim, “Estimating the unconfined compression strength of low plastic clayey soils using gene-expression programming,” *Geomechanics and Engineering*, vol. 33, no. 1, pp. 1–9, 2023.
- [16] A. F. Cabalar, S. O. Hama, and S. Demir, “Behaviour of a clay and gravel mixture,” *The Baltic Journal of Road and Bridge Engineering*, vol. 17, no. 1, pp. 98–116, 2022.
- [17] A. F. Cabalar and R. A. Hasan, “Compressional behaviour of various size/shape sand–clay mixtures with different pore fluids,” *Engineering Geology*, vol. 164, pp. 36–49, 2013.
- [18] S. Thevanayagam, “Effect of fines and confining stress on undrained shear strength of silty sands,” *Journal of Geotechnical and Geoenvironmental Engineering*, vol. 124, no. 6, Article ID 479, 1998.
- [19] N. Ecemis and M. Karaman, “Influence of non-/low plastic fines on cone penetration and liquefaction resistance,” *Engineering Geology*, vol. 181, pp. 48–57, 2014.
- [20] M. M. Monkul and G. Ozden, “Compressional behavior of clayey sand and transition fines content,” *Engineering Geology*, vol. 89, no. 3-4, pp. 195–205, 2007.
- [21] Z. Kong, Y. Guo, S. Mao, and W. Zhang, “Experimental study on shear strength parameters of round gravel soils in plateau alluvial–lacustrine deposits and its application,” *Sustainability*, vol. 15, no. 5, Article ID 3954, 2023.
- [22] W.-J. Chang and T. Phantachang, “Effects of gravel content on shear resistance of gravelly soils,” *Engineering Geology*, vol. 207, pp. 78–90, 2016.
- [23] K. Tang, X. Xie, and L. Yang, “Research on mechanical characteristics of gravel soil based on large-scale triaxial tests,” *Chinese Journal of Underground Space and Engineering*, vol. 10, no. 3, pp. 580–585, 2014.
- [24] J. Zhang, *Combination Modeling and Zone Partition Study on the Construction Area along Nanning’s Subway No. 1*, Guangxi University, 2012.
- [25] Nanning Rail Transit Group Co., Ltd, “Technical specification of retaining and protecting for building foundation excavation,” Local standard of Guangxi Engineering Construction (DBJ/T45-065-2018) China, 2018.
- [26] S. Pan, “The characteristics and significance of neotectonics in Nanning City,” *Geology of Guangxi*, vol. 13, no. 1, pp. 11–15, 2000.
- [27] X. Yan, *Study on the Deformation and Origin of the Third Terrace in Nanning Basin*, Guilin University of Technology, 2010.
- [28] Beijing Municipal Commission of Urban Planning, “Code for geotechnical investigations of urban rail transit,” National Standard of the PRC (GB 50307-2012), 2012.
- [29] Ministry of Water Resources of the PRC, “Standard for geotechnical testing method,” National Standard of the PRC (GB/T 50123-2019), 2019.
- [30] W. Hassan, M. F. Raza, B. Alshameri, A. Shahzad, M. H. Khalid, and M. N. Nawaz, “Statistical interpolation and spatial mapping of geotechnical soil parameters of District Sargodha, Pakistan,” *Bulletin of Engineering Geology and the Environment*, vol. 82, Article ID 37, 2023.
- [31] W. Hassan, B. Alshameri, M. N. Nawaz, Z. Ijaz, and M. Qasim, “Geospatial and statistical interpolation of geotechnical data for modeling zonation maps of Islamabad, Pakistan,” *Environmental Earth Sciences*, vol. 81, Article ID 547, 2022.
- [32] Ministry of Construction of the PRC, “Code for investigation of geotechnical engineering,” National Standard of the PRC (GB 50021-2001), 2001.
- [33] M. Wei, L.-C. Su, G.-H. Liang, S.-X. Li, and G.-Y. Zhou, “Field case of foundation pit construction of scientific building of Guangxi bureau of geology and mineral,” *Drilling Engineering*, no. 8, pp. 11–16, 2006.
- [34] J. Wu, *Analysis of the Interaction of High-Building Foundation and Short Piles on the Basis of Stratigraphic Combination in Nanning*, Guangxi University, 2007.
- [35] Y. Mai, *Comparative Research on the Design and Site Monitoring of Continuous Diaphragm Walls in Nanning—A Study of the Foundation Pit Engineering in Xiguan Plaza*, Guangxi University, 2012.
- [36] Z. Huang and L. Yang, “Option assessment of retaining structures and statistic analysis of stability coefficients for pit excavation in round gravels,” *Journal of Engineering Geology*, vol. 21, no. 3, pp. 438–442, 2013.
- [37] G. Zhou, “Bearing capacity of pile groups with solid rock soil layer at pile end,” *Guangxi Civil Engineering Architecture*, vol. 22, no. 2, pp. 47–52, 1997.